Bedrock detection based on seismic interferometry using ambient noise in Singapore

*Enhedelihai Nilot**, *Yunyue Elita Li**, *Karen Lythgoe*†
**Department of Civil & Environmental Engineering, National University of Singapore, Singapore*
†*Earth Observatory of Singapore, Nanyang Technological University, Singapore*

SUMMARY

The city-state of Singapore principally sits on granite bedrock known as the Bukit Timah formation. The Bukit Timah granite outcrops in the centre of Singapore, but it is buried below quaternary sediments known as the Old Alluvium formation in the east and north. Bedrock depth and faults in the shallow surface influence the stability of structures built above it, while the depth to bedrock constrains the water storage capacity and sub-soil water movement. Seismic methods are needed to image bedrock depth, however explosive methods are forbidden in the densely populated urban environment of Singapore. Passive seismic based on seismic interferometry is non-destructive and can provide us estimated detection depth. We apply the passive surface wave method based on seismic interferometry to the whole of Singapore island using a 1 month deployment of short-period nodes, to obtain the 3D velocity structure. We also obtain more detailed information in the Old Alluvium sediments by applying the MASW (multi-channel analysis of surface waves) method to linear geophone arrays. By analyzing the results from both tomography and MASW, we show that the granite bedrock beneath the Old Alluvium sediments is deeper than existing geological model suggests, which potentially increases the storage volume for fresh water in the deep underground acquifer.

INTRODUCTION

As more fresh water is needed to support rapidly expanding city populations, water storage to support a mega-city like Singapore is a significant challenge. Singapore has been investing in research and development to create alternative sources of fresh water for many years. However storage of fresh water remains a problem, and due to limited space above ground, the preferred solution is to develop an underground aquifer to store excess surface water. In order to fully evaluate the feasibility and to better plan for space utilization, appropriate geophysical subsurface mapping and characterization technologies are needed to map out the subsurface velocity of the whole island. However, in densely populated areas, electromagnetics methods often provide poor results primarily due to strong electromagnetic interferences, high human-related noises, and hence poor data quality and vertical resolution. Reflection and refraction seismic method can provide us the bedrock structural information based on P-wave velocity (Schmelzbach et al., 2005; Sheng et al., 2006). However, due to the "blindness" of refractions to slow formations and the limited resolution of the P-wave data, seismic reflection and refraction methods cannot resolve near-surface structure to the desired requirements of geological and civil engineers. Moreover, in the densely populated urban area, strong active sources with long geophone arrays for reflection and refraction measurements are not practical, thus the detection depth is very limited.

Alternatively, surface wave measurements are commonly utilized to resolve shear wave velocity and the near-surface structures. Due to the non-intrusive nature and relatively large detection depth, surface wave imaging has attracted increasing applications in urban environments (Nazarian et al., 1983; Park et al., 1999; Xia et al., 1999; Kanlı et al., 2006). In the surface wave measurement, its dispersive properties can be used to obtain important information about near-surface elastic properties. However, when the target layer is buried deep (over 100 m), the low frequency energy generated by an active source is not sufficient to provide information with good signal-to-noise ratio. Besides, because of the strict regulations on urban environment, the geophysical methods based on active methods are limited. Thus, the passive surface wave analysis method will be a better choice for the deep target detection in urban environment (Zhang et al., 2019b,a). Using seismic interferometry, empirical Green's functions (noise correlation functions), that are often dominated by Rayleigh waves on land, can be obtained. The shear wave velocity can then be recovered by analyzing the dispersion curve obtained from the noise correlation function.

Short period surface waves (1s to 15 s) have been used to investigate shallow crustal structure and for fault detection (Yao et al., 2005; Stehly et al., 2006; Yao et al., 2006; Huang et al., 2010; Green et al., 2017). In this frequency band, the main noise sources are believed to be loads caused by pressure perturbations in the atmosphere and the ocean (Stehly et al., 2006). For ambient noise above 1 Hz, the signals mainly originate from traffic and human activities. In this frequency range, passive surface wave methods have been applied in the detection of bedrock and civil engineering applications in urban environments (Park and Miller, 2008; Cheng et al., 2015; Clements and Denolle, 2018). Here, we aim to map the shear wave velocity structure of Singapore island, from the surface to below 1 km. Previous studies have measured that the depth to bedrock for the Jurong and Bukit Timah Formations (Zhang et al., 2019b,a), however these are for a few discrete points and no work has yet been done on the whole of Singapore island.We first use tomography based on passive surface wave analysis (in 0.5 - 4 s period range) in order to detect the bedrock depth and evaluate the potential water storage over Singapore island. We then complete higher frequency multi-channel analysis of surface wave (MASW, 0.1 - 0.5 s period range) to provide higher resolution detection of bedrock depth in the east of Singapore.

METHODOLOGY

Rayleigh waves result from interfering P- and SV- waves and have the strongest amplitude in the seismic profile (Aki and Richards, 2002). Rayleigh waves become dispersive when their wavelengths are in the range of 1-30 times the layer thickness. The noise correlation function (NCF) is an estimation of the earth response between two stations and S-wave velocity structures can be obtained by analysing their dispersion curves. The complete workflow of passive seismic processing can be divided into four principle parts (Bensen et al., 2007; Cheng et al., 2015), beginning with pre-processing. We remove the instrument response, bandpass filter, notch filter, apply temporal normalization and spectral whitening. Then, NCFs are derived from cross-correlation functions between all station pairs using the continuous vertical component of ambient noise:

$$G(x_2, x_1, \omega) = \sum_{n=1}^{N} U(x_2, x_s, \omega)\, U'(x_1, x_s, \omega) \qquad (1)$$

where $U(x_2, x_s, \omega)$ stands for the wavefield excited at x_s and received by receiver R_2 at location x_2, $U'(x_1, x_s, \omega)$ is of the complex conjugate of the wavefield excited at x_s and received by receiver R_1 at location x_1. The cross-correlation of observations at two receivers approximates the response between the two receivers where R_2 can be regarded as a virtual source. The cross-correlograms of all short time windows N are stacked together to improve the signal-to-noise ratio of the estimated Green's function. In the observation, we split the data into 1 hour's segment for pre-processing and 5 min data for cross-correlation for the short period seismometers. For each period (T) of interest we use a period-dependent (tapered) boxcar window between group velocities $[v_1(T)v_2(T)]$to window the NCF in the time domain; subsequently, the windowed NCFs for that period of interest is narrow-bandpass filtered using the group-velocity image-analysis technique (Yao et al., 2006). For the multi-channel arrays, we split the 1 hour multi-channel data into 10 second's segments and use frequency domain slant stack to get the phase velocity. After obtaining dispersion curves, we apply 3D surface wave tomography (Fang et al., 2015) and 1D PSO based dispersion curve inversion (Nilot et al., 2019) to get the shear wave velocity of whole island and the eastern part, respectively.

DATA AND PROCESSING

The outcrop of Singapore island is composed of three distinct geological formations: Jurong Formation of meta-sediments in the south and south-west, the Bukit Timah granite Formation in the north-central part, and the Old Alluvium Formation of Quaternary sediment in the east. An array of faults and fractures are developed in Singapore and they control bedrock unit distribution (Figure 1). The Bukit Timah Formation underlies the Old Alluvium in the east, however the Bukit Timah fault is a significant fault which separates the Jurong and Bukit Timah formations (Lythgoe et al., 2020). The depth to bedrock is 50 m or less for the Jurong and Bukit Timah formations, while it varies from 80 m to over 200 m for the Old Alluvium (Zhang et al., 2018, 2019a,b; Nilot et al., 2019).

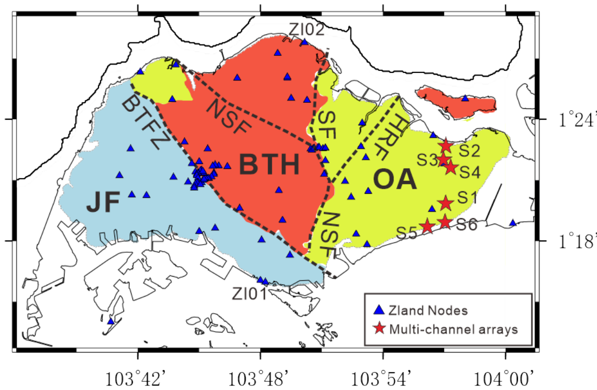

Figure 1: Tectonic units and major faults in Singapore. The main tectonic units are: JF (Jurong Formation), BTF (Bukit Timah Formation), OA (Old Alluvium Formation). The main faults are: BTFZ (The Bukit Timah Fault Zone), SF (Seletar Fault), NSF(Nee Soon Fault), HRF (Henderson Road Fault). Blue triangles indicates the location of short period seismometers, and red stars indicate sites for multi-channel geophones.

Continuous seismic records including both noise data and teleseismic earthquake data (e.g. Lythgoe et al. (2020)) were collected from 81 short period Z-Land nodes across Singapore and 6 multi-channel arrays in eastern Singapore (Figure 1). The Z-Land data is observed continuously from 2019/03/01 to 2019/04/01, while for the multi-channel arrays, the observation time is 1 hour or more. For the Z-Land nodes, there are a total of 3,240 station pairs, among which 936 (28.9%) are in a distance range between 0.2km-5km, 622 (19.2%) between 5km-10km and 622 (32.8%) between 10km-15km. Most previous ambient noise tomography work concentrates on periods higher than 5 s, but we use higher frequencies as we are more focused on the shallow geological structure. Our interstation distance is relatively short, so it is possible to use a relatively high frequency in ambient seismic noise tomography (Huang et al., 2010). We define signal-to-noise ratio (SNR) as the ratio between the maximum amplitude and average amplitude for each NCF. We plot all the cross-correlation functions with a SNR higher than 20 and arrange them by interstation distances in Figure 2. The final stacked NCFs in the period between 0.5 s-2 s, 2 s-5 s show a clear Rayleigh wave packet travels in a velocity between 1.5km/s to 4 km/s. From the total number of 3,240 station pairs, cross-correlation functions with a SNR higher than 20 are 139 (4.29%), 775 (23.92%), 934 (28.83%) and 71 (2.19%) for periods 0.1-0.5 s, 0.5-2 s, 2-5 s and 5-8 s, respectively. This means that signals with periods between 0.5-5 s have the relatively strongest energy. For each stack, amplitudes of the causal and anti-causal parts were determined by taking the maximum of their envelopes in a time window corresponding to the Rayleigh wave group velocity (Figure 3). The NCFs typically show strong asymmetry, which is the result of the anisotropic distribution of noise sources. Analysis of the variation of normalized amplitude with azimuth shows that the directions of the main noise sources are inconsistent in different frequency bands: for the period 0.5-2 s, energy from southwest and southeast is dominant, while for the period 2-5s, energy from the northeast is strongest (Figure 4).

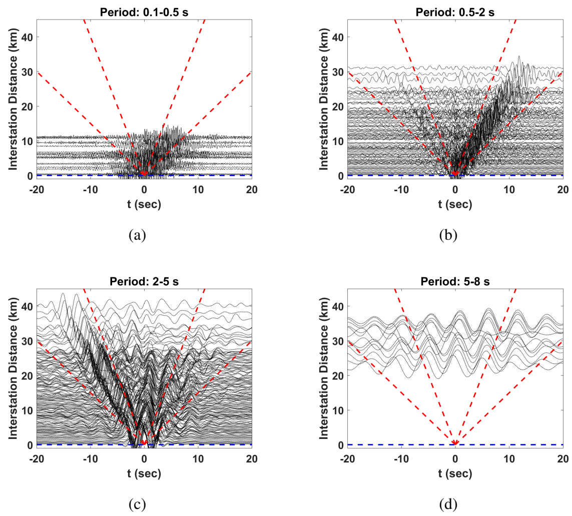

Figure 2: Extraction of Rayleigh waves. 30-day stacked Noice Correlation Function (a) 0.1-0.5s period (b) 0.5-2s period (c) 2-5s period (d) 5-8s period. The red dotted lines are 1.5 km/s and 4 km/s, respectively.

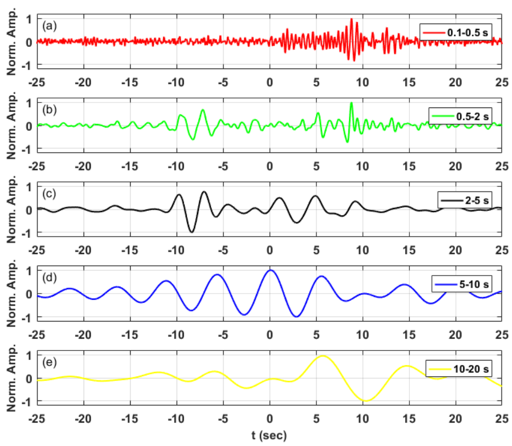

Figure 3: Noice Correlation Functions of station pair ZL01–ZL02 in the period of (a) 0.1-0.5 s (b) 0.5-2 s (c) 2-5 s (d) 5-10 s (e) 10-20 s.

The input data for surface wave tomography is the group travel times curves between station pairs (Figure 6). A total of 796 travel time paths at periods between 0.5-4 s are used to construct a group velocity map. The study region is meshed with 50*50*30 grid with an interval of 0.0058° in latitude and 0.009° in longitude and 0.05 km spacing in depth. The total iteration number is 20, which is sufficient for the model to converge and achieve a good fit to the short-period data.

Figure 6 shows the regional shear wave velocity model at depths

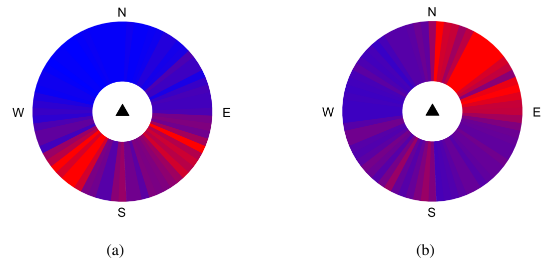

Figure 4: Normalized amplitude of the cross correlation averaged versus azimuth for various frequency bands (a) 0.5–2 s, (b) 2–5 s.

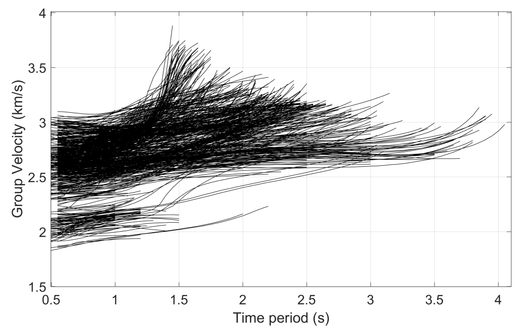

Figure 5: Dispersion curves of group velocity.

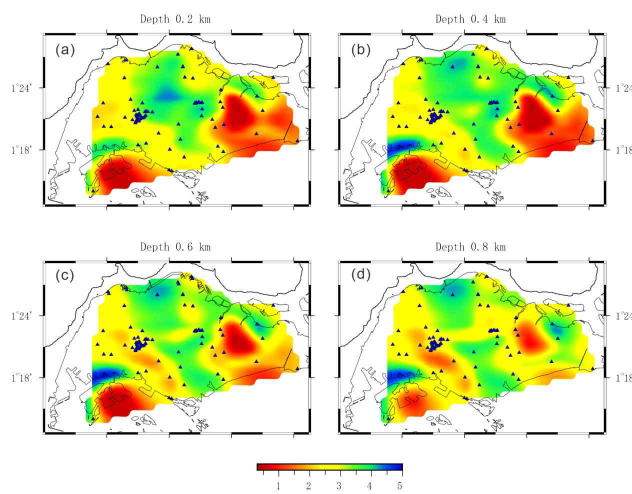

Figure 6: Horizontal slices of our tomography model in the depth of (a) 0.2 km (b) 0.4 km (c) 0.6 km (d) 0.8 km.

of 0.2, 0.4, 0.6 and 0.8 km respectively. The central part of Singapore has a the highest shallow shear wave velocity due to the shallow granite bedrock. Bukit Timah Fault zone appears as a local low-speed anomaly. Low shear wave velocity regions appear in the eastern part, which are dominated by Quaternary sediments in the shallow subsurface. Our principle noise sources for tomography are from ocean waves, and we cannot obtain reliable results at higher frequencies (such as periods of 0.1 - 0.5 s). Additionally, in eastern Singapore we have insufficient ray coverage to cover the whole Old Alluvium formation.

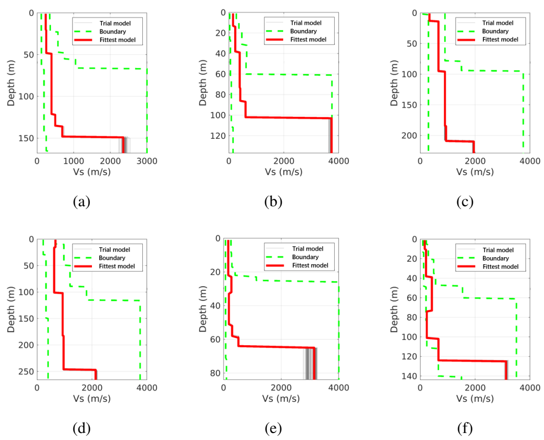

Figure 7: 1D inversion results from MASW at several sites in eastern Singapore. (a) site 1 (b) site 2 (c) site 3 (d) site 4 (e) site 5 (f) site 6.

The Old Alluvium is a semi-consolidated deposit, mainly composed of coarse sand, fine gravel and lenses of silt and clay. It is deposited on a basement of granitic and metamorphic rocks, and there exists a very high permeability layer at soil-rock interface (Pitts, 1984). The deep bedrock depth beneath the Old Alluvium suggests that the Old Alluvium formation is a good location for injecting and storing large amounts of fresh water. In order to improve our vertical resolution below the Old Alluvium formation, we deploy multi-channel linear arrays at 6 sites. In this application, the ambient noise energy is mainly concentrated in the frequency band of 2-10 Hz which is dominated by traffic noise and human activity. This supports an optimal linear acquisition geometry orthogonal to the major road in the study area.

Shear velocity inversion is performed by fitting the modeled dispersion curve with one picked from the data. We focus our attention on inversion results of fundamental-mode dispersion curves for layer thicknesses and surface wave velocities by fixing P-wave velocities and densities. When the velocity is larger than 2000 m/s, we identify the layer as the bedrock. In our 1D inversion results, the bedrock and upper layer sediments have a strong contrast and the bedrock depth is more than 100 m at most of the sites (Figure 7). We arrange the inversion results by site location from north to south in Table 1. Our inverted 1D velocity models are very similar to borehole log data at most sites. In the coastal area, the depth to bedrock is relatively shallow. However the bedrock could be very deep inland, particularly in the northern part of the formation.

	Borehole Depth	Inversion Depth	Distance
Site2	115m	103m	300m
Site3	200m	208m	30m
Site4	200m	245m	720m
Site1	110m	150m	400m
Site5	>145m	65m	96m
Site6	120m	124m	284m

Table 1: Bedrock depth from 1D inversion of surface wave dispersion and nearby boreholes. Borehole Depth is the bedrock depth obtained from borehole data, Inversion Depth is the bedrock depth from 1D dispersion inversion, Distance is the distance between the multi-channel array and the borehole.

CONCLUSIONS

In this study, we performed ambient seismic noise tomography at very short periods (0.5–4 s) across Singapore island, which has high ambient seismic noise levels due to natural and human activity. By picking group velocity from NCFs for tomography, we show that in the shallow crust of the Singapore island, the east region has a relatively lower shear wave velocity than other part. In other words, in this region, the depth to bedrock is relatively deeper than other part. By analysing the variation of amplitude versus azimuth, we conclude that the dominant noise source for period 0.5-2 s is mostly from the southeast and southwest directions, while for the period 2-5 s, the energy principally comes from the northeast. Our tomography model shows a low shear wave velocity in eastern Singapore, indicating that the bedrock depth is deepest here. For getting a more detailed shallow subsurface structures of eastern Singapore, we also obtained 6 multi-channel observation in the period of 0.1-0.5s. Our 1D inversion results show that the bedrock depth can be at least 270 m. The high permeability and deep bedrock indicates the Old Alluvium formation in eastern Singapore is a candidate for storage of large volumes of excess surface water in a deep underground aquifer.

ACKNOWLEDGMENTS

The authors acknowledge EDB Petroleum Engineering Professorship and Karen Lythgoe is funded by an NTU Presidential Fellowship.

REFERENCES

Aki, K., and P. G. Richards, 2002, Quantitative seismology.

Bensen, G., M. Ritzwoller, M. Barmin, A. L. Levshin, F. Lin, M. Moschetti, N. Shapiro, and Y. Yang, 2007, Processing seismic ambient noise data to obtain reliable broad-band surface wave dispersion measurements: Geophysical Journal International, **169**, 1239–1260.

Cheng, F., J. Xia, Y. Xu, Z. Xu, and Y. Pan, 2015, A new passive seismic method based on seismic interferometry and multichannel analysis of surface waves: Journal of applied geophysics, **117**, 126–135.

Clements, T., and M. A. Denolle, 2018, Tracking groundwater levels using the ambient seismic field: Geophysical Research Letters, **45**, 6459–6465.

Fang, H., H. Yao, H. Zhang, Y.-C. Huang, and R. D. van der Hilst, 2015, Direct inversion of surface wave dispersion for three-dimensional shallow crustal structure based on ray tracing: methodology and application: Geophysical Journal International, **201**, 1251–1263.

Green, R. G., K. F. Priestley, and R. S. White, 2017, Ambient noise tomography reveals upper crustal structure of icelandic rifts: Earth and Planetary Science Letters, **466**, 20–31.

Huang, Y.-C., H. Yao, B.-S. Huang, R. D. van der Hilst, K.-L. Wen, W.-G. Huang, and C.-H. Chen, 2010, Phase velocity variation at periods of 0.5–3 seconds in the taipei basin of taiwan from correlation of ambient seismic noise: Bulletin of the Seismological Society of America, **100**, 2250–2263.

Kanlı, A. I., P. Tildy, Z. Prónay, A. Pınar, and L. Hermann, 2006, Vs 30 mapping and soil classification for seismic site effect evaluation in dinar region, sw turkey: Geophysical Journal International, **165**, 223–235.

Lythgoe, K. H., M. O. S. Qing, and S. Wei, 2020, Large-scale crustal structure beneath singapore using receiver functions from a dense urban nodal array: Geophysical Research Letters.

Nazarian, S., I. Stokoe, H. Kenneth, and W. Hudson, 1983, Use of spectral analysis of surface waves method for determination of moduli and thicknesses of pavement systems.

Nilot, E., Y. Zhang, Y. E. Li, and X. Feng, 2019, Deep bedrock detection based on ambient noise recorded by a short geophone array: A singapore case study, *in* SEG Technical Program Expanded Abstracts 2019: Society of Exploration Geophysicists, 3121–3125.

Park, C. B., and R. D. Miller, 2008, Roadside passive multichannel analysis of surface waves (masw): Journal of Environmental and Engineering Geophysics, **13**, 1–11.

Park, C. B., R. D. Miller, and J. Xia, 1999, Multichannel analysis of surface waves: Geophysics, **64**, 800–808.

Pitts, J., 1984, A review of geology and engineering geology in singapore: Quarterly Journal of Engineering Geology and Hydrogeology, **17**, 93–101.

Schmelzbach, C., A. Green, and H. Horstmeyer, 2005, Ultra-shallow seismic reflection imaging in a region characterized by high source-generated noise: Near Surface Geophysics, **3**, 33–46.

Sheng, J., A. Leeds, M. Buddensiek, and G. T. Schuster, 2006, Early arrival waveform tomography on near-surface refraction data: Geophysics, **71**, U47–U57.

Stehly, L., M. Campillo, and N. Shapiro, 2006, A study of the seismic noise from its long-range correlation properties: Journal of Geophysical Research: Solid Earth, **111**.

Xia, J., R. D. Miller, and C. B. Park, 1999, Estimation of near-surface shear-wave velocity by inversion of rayleigh waves: Geophysics, **64**, 691–700.

Yao, H., R. D. van Der Hilst, and M. V. De Hoop, 2006, Surface-wave array tomography in se tibet from ambient seismic noise and two-station analysis—i. phase velocity maps: Geophysical Journal International, **166**, 732–744.

Yao, H., G. Xu, L. Zhu, and X. Xiao, 2005, Mantle structure from inter-station rayleigh wave dispersion and its tectonic implication in western china and neighboring regions: Physics of the Earth and Planetary Interiors, **148**, 39–54.

Zhang, Y., Y. E. Li, and T. Ku, 2019a, *in* Near-surface bedrock profiling using urban ambient noise: An autocorrelation approach: Society of Exploration Geophysicists, 3126–3130.

Zhang, Y., Y. E. Li, and H. Zhang, 2019b, Near-surface site investigation by seismic interferometry using urban traffic noise in singapore: Geophysics, **84**, B169–B180.

Zhang, Y., Y. E. Li, H. Zhang, and T. Ku, 2018, *in* Optimized passive seismic interferometry for bedrock detection: A Singapore case study: Society of Exploration Geophysicists, 2506–2510.